King Saud University

Arabian Journal of Chemistry

ORIGINAL ARTICLE

Irregularity molecular descriptors of Cerium oxide CeO_2 based on mathematical model and calculation

Qi Zhang [a], **Muhammad Mobeen Munir** [b,*], **Haseeb Ahmad** [c], **Jia-Bao Liu** [d]

[a] *College of Mathematics and Computer Science, Tongling University, Anhui 244000, PR China*
[b] *Department of Mathematics, University of the Punjab, Lahore 54500, Pakistan*
[c] *Division of Science and Technology, University of Education, Lahore 54000, Pakistan*
[d] *School of Mathematics and Physics, Anhui Jianzhu University, Hefei 230601, PR China*

Abstract The irregularities of graphs and their dependencies on the size parameters are recently attracting attention of not only mathematician but also of theoretical chemists. It is found that these irregularities are related with the properties of the substance involved. Cerium oxide is a rare-earth metal having formula CeO_2 and it is light yellow-white powder. In the present article we are concerned with computing the closed forms of irregularity measures of general form of crystal structure of Cerium Oxide CeO_2 based on mathematical model and calculation.

1. Introduction

Chemical Graph Theory is recently flourishing because of increasing number of structural dependent functions which exhibit the topological aspects of the chemical substance under consideration. Physio-chemical aspects of the materials are related to these functions in a complex way. Topological degree-based descriptors are numerical estimators which relate these properties. One class of such descriptors is irregularity measure which computes the complexity of the chemical structures. This degree of complexity determines the degree of

chemical branching and bonding pattern, enthalpy, stability and strain energy, (Abdo and Dimitrov, 2014; Gutman, 2018; Reti et al., 2018; Hu et al., 2005). The present article computes irregularity measures of Cerium oxide in closed analytic form.

Basic structure of cerium oxide is such that each cerium ion Ce^{4+} is surrounded by eight oxide ions O_2 that forms a cubic shape molecule and each oxide ion is enclosed by four Ce^{4+} ions which forms a tetrahedron molecule (Sayle et al., 1994). This structure is rich in exceptional physical and chemical properties. Its optical and electrical properties are generally because of the little size and huge thickness of corners. Cerium exists both in CeO_2 and Ce_2O_3 in bulk state as demonstrated in Fig. 2. This double oxide nature is because of the electropositive qualities of ceria, Ce_2O_3, also called the "sesquioxide", Fig. 3. The magnetic property is profoundly temperature dependent. This property is not present in the large structure as it has only + 4 state (Ribeiro and Ferreira, 2017). Every strange and special property of cerium oxide is

E-mail addresses: zhangqi830917@163.com (Q. Zhang), mmunir.math@pu.edu.pk (M.M. Munir), liujiabaoad@163.com (J.-B. Liu).
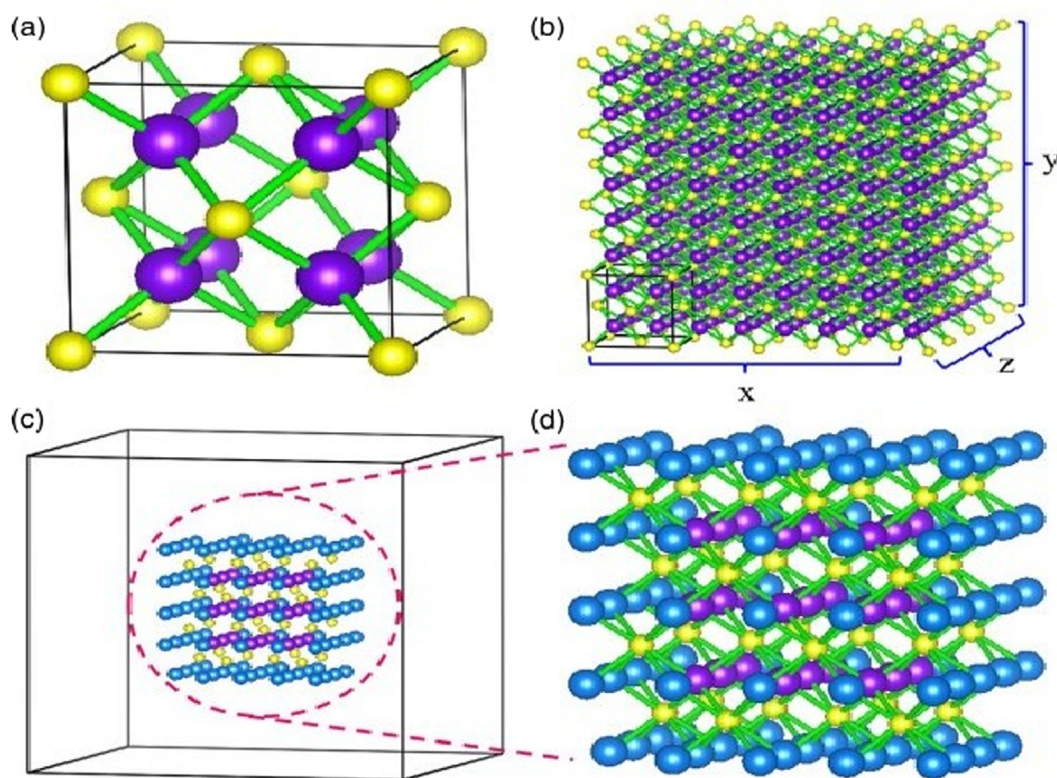
Fig. 1 Part (a) shows the unit cell of bulkCeO₂, part (b) shows schematic illustration of building the solid atomic assembly of Ce (cerium) and O (oxygen) atoms by randomly expanding the unit cell of bulk CeO₂ (enclosed by black solid lines) ×, y, and z times in three orthonormal directions, respectively part (c) the super cell of cubic cerium oxide nanoparticles of 1 nm for relaxation calculation (d) zoom-in picture of the solid atomic assembly in part c.
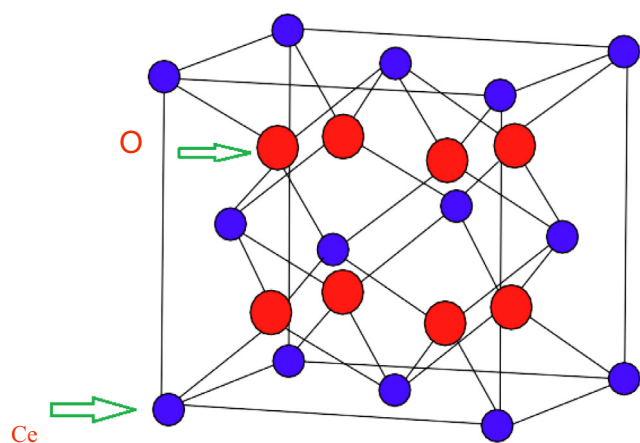

Fig. 2 Unit cell of.CeO₂

Fig. 3 Graph of irregularity index IRDIF.

because of the oxygen vacancy. In Cerium oxide a stable structure is due to the high oxygen storage capacity. When the size of cerium material is small, these oxygen vacancies tend to increase (Tseng et al., 2019; Wu et al., 2018).

Topological index is one such rich area of mathematics where it can enter in chemistry and bring revolution in determining properties of the chemical substances (Rucker and Rucker, 1999; Klavžar and Gutman, 1996; Brückler et al., 2011; Deng et al., 2011). The basic branch involved is the Chemical Graph Theory. In order to move on, we need to
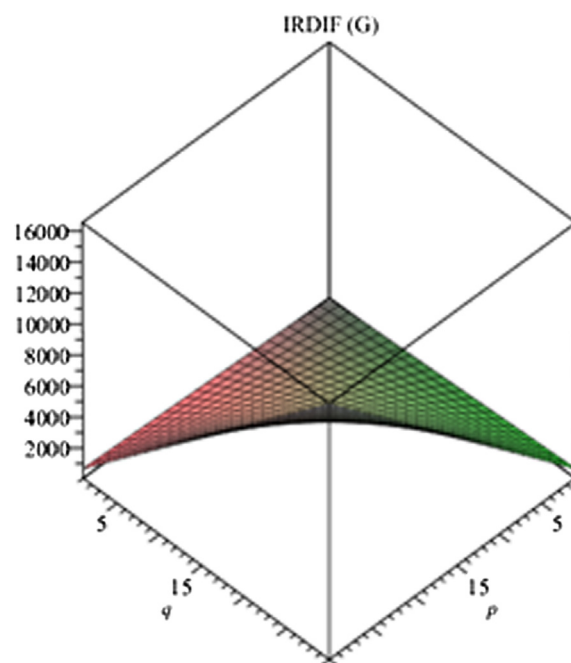
grasp some rudiments of Graph Theory. Let us denote G to be a simple connected graph having vertex set V and edge set E. Let us fix d_u and d_v for the degrees of vertices u and

v respectively. A graph is known to be regular if every vertex of the graph has the same degree. A topological invariant is called an irregularity index if this index vanishes for a regular graph, and remains non-zero for otherwise. Regular graphs are technically nicer than irregular ones and consequently have been extensively investigated, particularly in mathematics. After the discoveries of nanotubes and fullerenes, the regular graphs became more popular especially in Chemical Graph Theory. Today it is well-established that the topology of fullerenes is rich and has potential of many applications in mathematics. However, the irregular graphs remained unnoticed for a long time.

Paul Erdos, the famous Hungarian mathematician, put a lot of emphasis on the study of irregular graphs for the first time in history in (Chartrand et al., 1988). He posed a problem in (1994), that what could be the extreme size of highly irregular graph of a given order, (Majcher and Michael, 1997). This problem in fact opened gates for mathematician to study irregular graphs and the degree of irregularity as well. A particular graph would be highly strange in which in which each vertex has a different degree. Such graphs were termed as perfect graphs. The authors of (Behzad and Chartrand, 1947) demonstrated that no graph is perfect. The graphs lying in between are called quasi-perfect graphs, in which all except two vertices have different degrees (Majcher and Michael, 1997). One way of expressing irregularities of graphs is the computation of irregularity indices. These indices can be based on many pieces of information such as degrees of vertices, eccentricities of vertices etc. Some irregularity indices were studied recently in a novel way (Horoldagva et al., 2016; Liu et al., 2014; Collatz and Sinogowitz, 1957). The first such irregularity index was introduced in (Bell, 1992). Most of these indices which are based on degree of vertices used the concept of the imbalance of an edge defined as $imball_{uv} = |du - dv|$; (Behzad and Chartrand, 1947; Horoldagva et al., 2016; Liu et al., 2014; Collatz and Sinogowitz, 1957; Bell, 1992; Albertson, 1997).

The Albertson index denoted by, AL(G), was initially introduced by Alberston in (Albertson, 1997) as $AL(G) = \sum_{UV \in E} |d_u - d_v|$. The irregularity index IRL(G) and IRLU(G) were introduced by Vukičević and Gasparov, (Vukičević and Graovac, 2004) as $IRL(G) = \sum_{UV \in E} |ln d_u - ln d_v|$, and $IRLU(G) = \sum_{UV \in E} \frac{|d_u - d_v|}{min(d_u, d_v)}$ where min is used as the minimum of the parameters given. Recently, Abdoo et al. defined the new term "total irregularity measure of a graph G", as $IRR_t(G) = \frac{1}{2} \sum_{UV \in E} |d_u - d_v|$, (Abdo et al., 2014; Abdo and Dimitrov, 2014; Abdo and Dimitrov, 2014). Recently, Gutman et al. introduced the IRF(G) irregularity index of the graph G, which is described as $IRF(G) = \sum_{UV \in E} (d_u - d_v)^2$ in (Gutman, 2018). Reti et al. discussed the relation of irregularity indices and properties in (Reti et al., 2018). The Randic index itself is directly related to an irregularity measure, which is described as $IRA(G) = \sum_{UV \in E} \left(d_u^{-\frac{1}{2}} - d_v^{-\frac{1}{2}} \right)^2$ in (Yang et al., 2019). Further irregularity indices of similar nature can be traced in (Gutman, 2018; Reti et al., 2018; Hu et al., 2005) in detail. These indices are given as $IRDIF(G) = \sum_{UV \in E} \left| \frac{d_u}{d_v} - \frac{d_v}{d_u} \right|$; $IRLF(G) = \sum_{UV \in E} \frac{|d_u - d_v|}{\sqrt{(d_u d_v)}}$; $LA(G) = 2 \sum_{UV \in E} \frac{|d_u - d_v|}{(d_u + d_v)}$, $IRD1 = \sum_{UV \in E} ln\{1 + |d_v - d_v|\}$, $IRGA(G) = \sum_{UV \in E} ln \frac{d_u + d_v}{2\sqrt{(d_u d_v)}}$, and $IRB(G) = $

$\sum_{UV \in E} \left(d_u^{\frac{1}{2}} - d_v^{\frac{1}{2}} \right)^2$. Further details can be given in (Gutman, 2018; Reti et al., 2018; Hu et al., 2005; Zahid et al., 2019; Gao et al., 2019; Gao et al., 2017; Hussain et al., 2019; Hussain et al., 2020; Yang et al., 2019; Hussain et al., 2019; Estrada, 2010 Sep). These irregularity measures have been put to use in determining an estimate of the properties of octane isomers in (Reti et al., 2018). Reti et al. actually did comparative regression analysis on the eighteen different irregularity indices of five different properties of octane isomers and concluded that these properties such as boiling point, standard enthalapy of vaporization, acentric factor, enthalapy of vaporization and entropy can be estimated with good accuracy of these isomers, (Reti et al., 2018). This side depict the actual applications of these indices. Other side of the story is to consider different matrices based on these irregularity indices and the eigen values of these matrices give us the energies related to these molecular graphs. These energies have deep applications in chemistry and physics such as to determine pi-electron energy. Authors in (Estrada, 2010 Sep) critically analyzed the irregularity of 10 protein–protein interaction networks in different organisms ranging from 50 to 3000 nodes. These indices can play helpful Job in estimating the properties of the molecular substances involved. Recently, Zahid et al. computed the irregularity indices of a nanotube (Zahid et al., 2019). Gao et al. recently computed irregularity measures of some dendrimer structures in (Gao et al., 2019) and molecular structures in (Gao et al., 2017). These structures are used as long infinite chain macromolecules in chemistry and related areas. Hussain et al. computed irregularities of different non-homeomorphic benzenoid structures in (Hussain et al., 2019; Hussain et al., 2020). Yang et al. discussed the imbalance-based irregularities of two types of boron nanotubes in (Yang et al., 2019). Hussain et al. also computed imbalance-based irregularities of nanostar dendrimers in (Hussain et al., 2019). As structures are rich in topology, so more and more investigations of irregular structures are in progress. In this article we focus on the topological structural facts of Cerium Oxide CeO_2. More precisely, we are interested in computing the imbalance-based degree of irregularity measures of general form of Cerium OxideCeO_2. Following Fig. 1 shows the topological structure of CeO_2.

In Cerium Oxide Ce atoms are shown by blue circles and oxygen O atoms are shown by red circles. In the CeO_2 unit cell, each Ce atom located at corner of a cube is coordinated with three Ce atoms, and one oxygen O atom, on other hand each Ce atom located at face of a cube is coordinated with four oxygen O atoms as shown in Fig. 2. Now in the next section we move towards our computational results. We also show some graphical analysis of the irregularities involved. It is worth mentioning that Cerium Oxide doped obsidian glasses are better radiation shielding materials than ordinary obsidian glass, as mass attenuation coefficients of CeO_2 doped obsidian glass decrease with increasing photon energy, (Yalcin et al., 2019). In (Yılmaz et al., 2020), authors computed some indices relating to the radiation shielding parameters like linear attenuation coefficients mass attenuation coefficients, effective atomic numbers, effective electron densities, half value of layers and mean free paths for rare earth metal oxides CeO_2 doped borosilicate (BS) glasses.

2. Main results

In this section, we present our main theoretical results. Following main result gives closed formulas for as many as twelve irregularity measures of $CeO_2[p, q, t]$.

Theorem:. *Let $CeO_2[p, q, t]$ be the crystal structure of Cerium Oxide. Tthen the irregularity indices of CeO_2 are:*

1. $IRDIF(CeO_2[p, q, t].) = 16.3pqt + 1.83pq + 1.83pt + 1.83qt + 1.6p + 1.6q + 1.6t + 9.83$
2. $AL(CeO_2[p, q, t].) = 40pqt + 4pq + 4pt + 4qt + 4p + 4q + 4t + 24.$
3. $IRL(CeO_2[p, q, t].) = 7.873pqt + 0.928pq + 0.928pt + 0.928qt + 0.8109p + 0.8109q + 0.8109t + 4.747797.$
4. $IRLF(CeO_2[p, q, t].) = 10pqt + pq + pt + qt + p + q + t + 6.$
5. $IRLU(CeO_2[p, q, t].) = 7.946182pqt + 0.9258pq + 0.9258pt + 0.9258qt + 0.816p + 0.816q + 0.816t + 4.78958.$
6. $IRF(CeO_2[p, q, t].) = 96pqt + 8p + 8q + 8t + 56.$
7. $IRLA(CeO_2[p, q, t].) = 7.73pqt + 0.933pq + 0.933pt + 0.933qt + 0.8p + 0.8q + 0.8t + 4.6667.$
8. $IRD1 = 20.796668pqt + 2.785pq + 2.785pt + 2.785qt + 2.1972p + 2.1972q + 2.1972t + 12.5955.$
9. $IRA(CeO_2[p, q, t].) = 0.17758pqt + 0.0122pq + 0.0122pt + 0.0122qt + 0.01683p + 0.01683q + 0.01683t + 0.105627.$
10. $IRGA(CeO_2[p, q, t].) = 3.61953pqt + 0.639pq + 0.639pt + 0.639qt + 0.4082p + 0.4082q + 0.4082t + 2.218017.$
11. $IRB(CeO_2[p, q, t].) = 4.60524pqt + 0.12187pq + 0.12187pt + 0.12187qt + 0.40408p + 0.40408q + 0.40408t + 2.7067.$
12. $IRR_t(CeO_2[p, q, t].) = 20pqt + 2pq + 2pt + 2qt + 2p + 2q + 2t + 12..$

Proof. *In order to prove the above theorem, we have to consider* Figs. 1 and 2 *from where some partitions of edge sets and vertex sets can be computed.*

Now, using above Table 1 and the above definitions, we have:

1. $IRDIF(G) = \sum_{UV \in E} \left| \frac{d_u}{d_v} - \frac{d_v}{d_v} \right|$

$IRDIF(CeO_2[p, q, t])$

$$= 16pqt + 4pq + 4pt + 4qt + 2p + 2q + 2t + 10\left|\frac{4}{4} - \frac{4}{4}\right|$$
$$+ 16pqt + 4pq + 4pt + 4qt + 2p + 2q + 2t + 10\left|\frac{6}{4} - \frac{4}{6}\right|$$
$$+ 2pqt - pq - pt - qt + 1\left|\frac{8}{4} - \frac{4}{8}\right| + 2pqt - pq - pt - qt$$
$$+ p + q + t - 2\left|\frac{6}{6} - \frac{6}{6}\right|$$

$$= 16pqt + 4pq + 4pt + 4qt + 2p + 2q + 2t + 10\left|\frac{6}{4} - \frac{4}{6}\right| + 2pqt$$
$$- pq - pt - qt + 1\left|\frac{8}{4} - \frac{4}{8}\right|$$

2. $AL(G) = \sum_{UV \in E} |d_u - d_v|$

$AL(CeO_2[p, q, t].)$

$$= 16pqt + 4pq + 4pt + 4qt + 2p + 2q + 2t + 10|4 - 4|$$
$$+ 16pqt + 4pq + 4pt + 4qt + 2p + 2q + 2t + 10|6 - 4|$$
$$+ 2pqt - pq - pt - qt + 1|8 - 4| + 2pqt - pq - pt - qt$$
$$+ p + q + t - 2|6 - 6|$$

$$= 40pqt + 4pq + 4pt + 4qt + 4p + 4q + 4t + 24$$

3. $IRL(G) = \sum_{UV \in E} |ln d_u - ln d_v|$

$IRL(CeO_2[p, q, t])$

$$= 16pqt + 4pq + 4pt + 4qt + 2p + 2q + 2t + 10|ln4 - ln4|$$
$$+ 16pqt + 4pq + 4pt + 4qt + 2p + 2q + 2t + 10|ln6 - ln4|$$
$$+ 2pqt - pq - pt - qt + 1|ln8 - ln4| + 2pqt - pq - pt - qt$$
$$+ p + q + t - 2|ln6 - ln6|$$

$$= (16pqt + 4pq + 4pt + 4qt + 2p + 2q + 2t + 10)ln\frac{6}{4}$$
$$+ (2pqt - pq - pt - qt + 1)ln\frac{8}{4}$$

4. $IRLU(G) = \sum_{UV \in E} \frac{|d_u - d_v|}{min(d_u, d_v)}$

$IRLU(CeO_2[p, q, t])$

$$= 16pqt + 4pq + 4pt + 4qt + 2p + 2q + 2t + 10\frac{|4 - 4|}{4}$$
$$+ 16pqt + 4pq + 4pt + 4qt + 2p + 2q + 2t + 10\frac{|6 - 4|}{4}$$
$$+ 2pqt - pq - pt - qt + 1\frac{|8 - 4|}{4} + 2pqt - pq - pt - qt$$
$$+ p + q + t - 2\frac{|6 - 6|}{6}$$

$$= (16pqt + 4pq + 4pt + 4qt + 2p + 2q + 2t + 10)\frac{1}{2} + (2pqt$$
$$- pq - pt - qt + 1)$$

5. $IRLF(G) = \sum_{UV \in E} \frac{|d_u - d_v|}{\sqrt{(d_u d_v)}}$

$IRLF(CeO_2[p, q, t])$

$$= 16pqt + 4pq + 4pt + 4qt + 2p + 2q + 2t + 10\frac{|4 - 4|}{\sqrt{16}}$$
$$+ 16pqt + 4pq + 4pt + 4qt + 2p + 2q + 2t + 10\frac{|6 - 4|}{\sqrt{24}}$$
$$+ 2pqt - pq - pt - qt + 1\frac{|8 - 4|}{\sqrt{32}} + 2pqt - pq - pt - qt$$
$$+ p + q + t - 2\frac{|6 - 6|}{\sqrt{36}}$$

$$= (16pqt + 4pq + 4pt + 4qt + 2p + 2q + 2t + 10)\frac{|2|}{\sqrt{24}}$$
$$+ (2pqt - pq - pt - qt + 1)\frac{|4|}{\sqrt{32}}$$

Table 1 Edge partition of Cerium Oxide beCeO_2.

Number of edges (d_u, d_v)	Number of indices
(4,4)	$16pqt + 4pq + 4pt + 4qt + 2p + 2q + 2t + 10$
(4,6)	$2pqt + 2pq + 2pt + 2qt - p - q - t - 5$
(4,8)	$2pqt - pq - pt - qt + 1$
(6,6)	$2pqt - pq - pt - qt + p + q + t - 2$

6. $IRF(G) = \sum_{UV \in E}(d_u - d_v)^2$

$IRF(CeO_2[p,q,t])$

$$= 16pqt + 4pq + 4pt + 4qt + 2p + 2q + 2t + 10(4-4)^2$$
$$+ 16pqt + 4pq + 4pt + 4qt + 2p + 2q + 2t + 10(6-4)^2$$
$$+ 2pqt - pq - pt - qt + 1(8-4)^2 + 2pqt - pq - pt - qt$$
$$+ p + q + t - 2(6-6)^2$$

$$= 96pqt + 8p + 8q + 8t + 56$$

7. $IRLA(G) = 2\sum_{UV \in E}\frac{|d_u - d_v|}{(d_u + d_v)}$

$IRLA(CeO_2[p,q,t])$

$$= 2\left[16pqt + 4pq + 4pt + 4qt + 2p + 2q + 2t + 10\frac{|4-4|}{8}\right.$$
$$+ 16pqt + 4pq + 4pt + 4qt + 2p + 2q + 2t + 10\frac{|6-4|}{10}$$
$$+ 2pqt - pq - pt - qt + 1\frac{|8-4|}{12} + 2pqt - pq - pt$$
$$\left. - qt + p + q + t - 2\frac{|6-6|}{12}\right]$$

$$= 2\left[(16pqt + 4pq + 4pt + 4qt + 2p + 2q + 2t + 10)\frac{2}{10}\right.$$
$$\left. + (2pqt - pq - pt - qt + 1)\frac{4}{12}\right]$$

8. $IRD1 = \sum_{UV \in E}ln\{1 + |d_v - d_v|\}$

$$IRD1 = 16pqt + 4pq + 4pt + 4qt + 2p + 2q + 2t + 10ln\{1$$
$$+ |4-4|\} + 16pqt + 4pq + 4pt + 4qt + 2p + 2q + 2t$$
$$+ 10ln\{1 + |6-4|\} + 2pqt - pq - pt - qt + 1ln\{1$$
$$+ |8-4|\} + 2pqt - pq - pt - qt + p + q + t - 2ln\{1$$
$$+ |6-6|\}$$

$$= (16pqt + 4pq + 4pt + 4qt + 2p + 2q + 2t + 10)ln(3) + (2pqt$$
$$- pq - pt - qt + 1)ln(5).$$

9. $IRA(G) = \sum_{UV \in E}\left(d_u^{\frac{-1}{2}} - d_v^{\frac{-1}{2}}\right)^2$

$IRA(CeO_2[p,q,t])$

$$= 16pqt + 4pq + 4pt + 4qt + 2p + 2q + 2t + 10\left(\frac{1}{\sqrt{4}} - \frac{1}{\sqrt{4}}\right)^2$$
$$+ 16pqt + 4pq + 4pt + 4qt + 2p + 2q + 2t + 10\left(\frac{1}{\sqrt{6}} - \frac{1}{\sqrt{4}}\right)^2$$
$$+ 2pqt - pq - pt - qt + 1\left(\frac{1}{\sqrt{8}} - \frac{1}{\sqrt{4}}\right)^2 + 2pqt - pq - pt$$
$$- qt + p + q + t - 2\left(\frac{1}{\sqrt{6}} - \frac{1}{\sqrt{6}}\right)^2$$

$$= 16pqt + 4pq + 4pt + 4qt + 2p + 2q + 2t + 10\left(\frac{1}{\sqrt{6}} - \frac{1}{\sqrt{4}}\right)^2$$
$$+ 2pqt - pq - pt - qt + 1\left(\frac{1}{\sqrt{8}} - \frac{1}{\sqrt{4}}\right)^2$$

10. $IRGA(G) = \sum_{UV \in E}ln\frac{d_u + d_v}{2\sqrt{(d_u d_v)}}$

Table 2 Irregularity indices for Cerium Oxide(CeO_2).

Irregularity Indices	p = 1, q = 1, t = 1	p = 2, q = 2, t = 2	p = 3, q = 3, t = 3	p = 4, q = 4, t = 4	p = 5, q = 5, t = 5
$IRDIF(G) = \sum_{UV \in E}\left|\frac{d_u}{d_v} - \frac{d_v}{d_u}\right|$	36.42	171.79	513.74	1160.07	2208.58
$AL(G) = \sum_{UV \in E}|d_u - d_v|$	88	416	1248	2824	5384
$IRL(G) = \sum_{UV \in E}|ln d_u - ln d_v|$	17.837497	83.733197	249.672897	562.894597	1070.636297
$IRLU(G) = \sum_{UV \in E}\frac{|d_u - d_r|}{min(d_u, d_r)}$	22	104	312	706	1342
$IRLU(G) = \sum_{UV \in E}\frac{|d_u - d_r|}{\sqrt{(d_u d_r)}}$	17.971162	84.364636	251.677097	567.575628	1097.737330
$IRF(G) = \sum_{UV \in E}(d_u - d_v)^2$	176	872	2720	6296	12,176
$IRLA(G) = 2\sum_{UV \in E}\frac{|d_u - d_r|}{(d_u + d_r)}$	17.6757	82.5027	245.7677	553.7707	1052.8917
$IRD1 = \sum_{UV \in E}ln\{1 + |d_v - d_v|\}$	48.3387	225.5720	669.07533	1503.6286	2854.0120
$IRA(G) = \sum_{UV \in E}\left(d_u^{\frac{-1}{2}} - d_v^{\frac{-1}{2}}\right)^2$	0.370297	1.367747	5.381157	12.258307	23.470577
$IRGA(G) = \sum_{UV \in E}ln\frac{d_u + d_v}{2\sqrt{(d_u d_v)}}$	8.979147	41.291457	120.872127	269.438337	508.707267
$IRB(G) = \sum_{UV \in E}\left(d_u^{\frac{1}{2}} - d_v^{\frac{1}{2}}\right)^2$	8.88909	43.43484	133.97469	308.14008	553.56245
$IRR_t(G) = \frac{1}{2}\sum_{UV \in E}|d_u - d_v|$	44	208	624	1412	2692

$IRGA(CeO_2[p,q,t])$

$$= (16pqt + 4pq + 4pt + 4qt + 2p + 2q + 2t + 10)ln\frac{|4-4|}{2\sqrt{16}}$$

$$+ (16pqt + 4pq + 4pt + 4qt + 2p + 2q + 2t + 10)ln\frac{|6-4|}{2\sqrt{24}}$$

$$+ (2pqt - pq - pt - qt + 1)ln\frac{|8-4|}{2\sqrt{32}}$$

$$+ (2pqt - pq - pt - qt + p + q + t - 2)ln\frac{|6-6|}{2\sqrt{36}}$$

$$= (16pqt + 4pq + 4pt + 4qt + 2p + 2q + 2t + 10)ln\frac{1}{\sqrt{24}}$$

$$+ (2pqt - pq - pt - qt + 1)ln\frac{2}{\sqrt{32}}$$

11. $IRB(G) = \sum_{UV \in E}\left(d_u^{\frac{1}{2}} - d_v^{\frac{1}{2}}\right)^2$

$IRB(CeO_2[p,q,t])$

$$= (16pqt + 4pq + 4pt + 4qt + 2p + 2q + 2t + 10)\left(\sqrt{4} - \sqrt{4}\right)^2$$

$$+ (16pqt + 4pq + 4pt + 4qt + 2p + 2q + 2t + 10)\left(\sqrt{6} - \sqrt{4}\right)^2$$

$$+ (2pqt - pq - pt - qt + 1)\left(\sqrt{8} - \sqrt{4}\right)^2$$

$$+ (2pqt - pq - pt - qt + p + q + t - 2)\left(\sqrt{6} - \sqrt{6}\right)^2$$

$$= (16pqt + 4pq + 4pt + 4qt + 2p + 2q + 2t + 10)\left(\sqrt{6} - \sqrt{4}\right)^2$$

$$+ (2pqt - pq - pt - qt + 1)\left(\sqrt{8} - \sqrt{4}\right)^2.$$

12. $IRR_t(G) = \frac{1}{2}\sum_{UV \in E}|d_u - d_v|$

Fig. 4   Graph of irregularity index AL.

$IRR_t(CeO_2[p,q,t])$

$$= \frac{1}{2}[16pqt + 4pq + 4pt + 4qt + 2p + 2q + 2t + 10|4-4|$$

$$+ 16pqt + 4pq + 4pt + 4qt + 2p + 2q + 2t + 10|6-4|$$

$$+ 2pqt - pq - pt - qt + 1|8-4| + 2pqt - pq - pt - qt$$

$$+ p + q + t - 2|6-6|]$$

$$= 20pqt + 2pq + 2pt + 2qt + 2p + 2q + 2t + 12.$$

Table 2. Shows the values of these irregularity indices for some test values of parameter p, q t.

3. Graphical analysis and discussions

Present part is devoted to the irregularity analysis of abovementioned Cerium Oxide(CeO_2). The graphs as indicated in
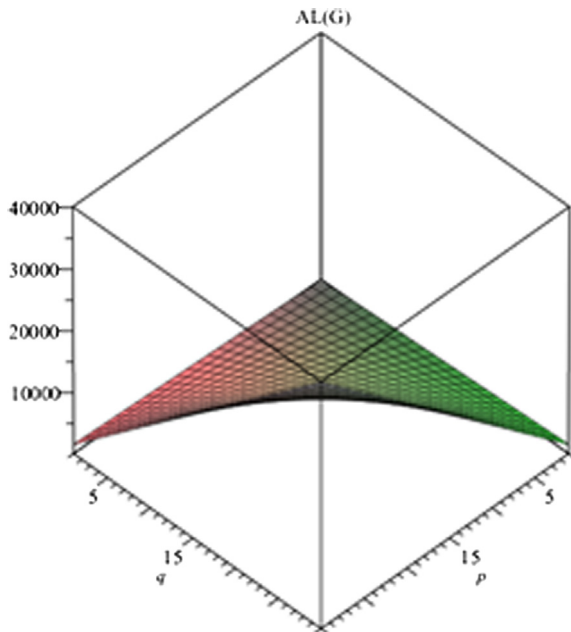
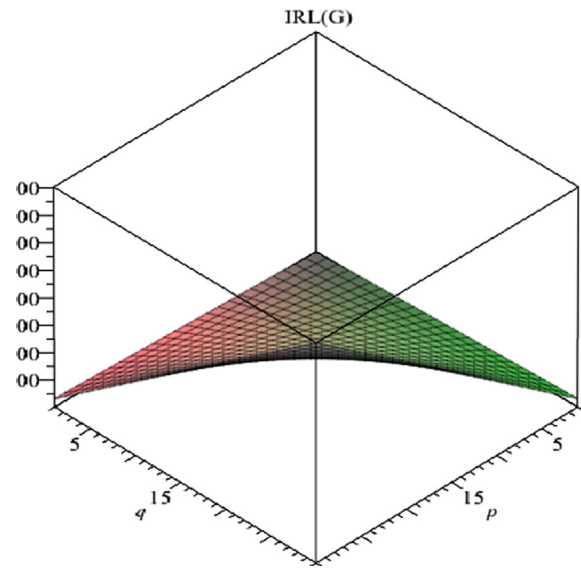

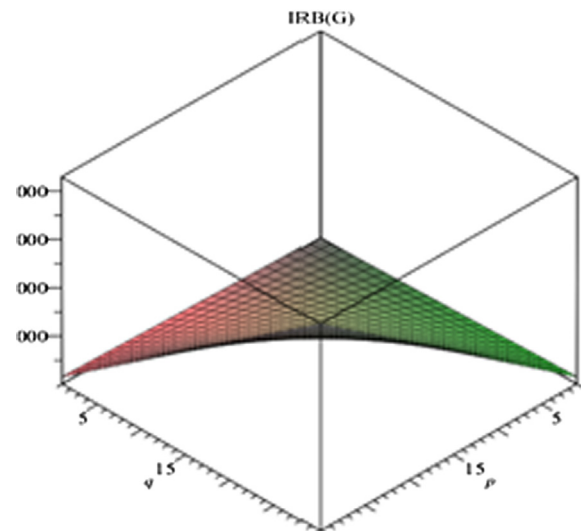**Fig. 5**   Graph of irregularity index IRL.

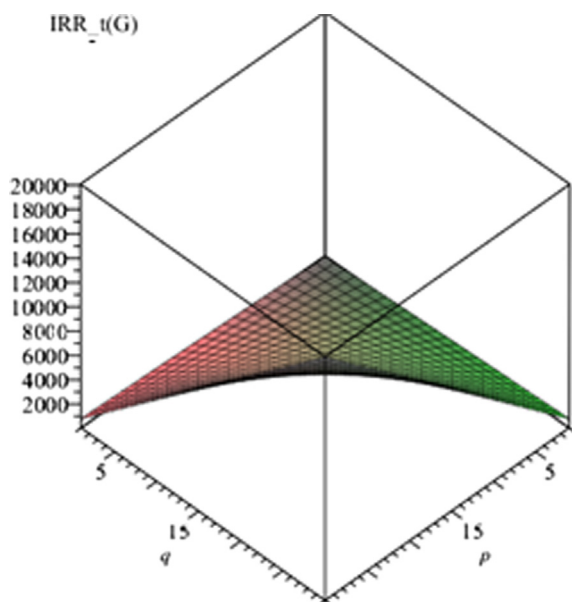**Fig. 6**   Graph of irregularity index IRB.

Fig. 7 Graph of irregularity index IRR_t cerium oxide when p, q are variables and t is fixed (t = 1) as shown in Figs. 4–7.

Figs. 4–7 show irregularity behavior of any particular index with respect to the parameters involved in the structure. In the present case, the involved parameters are p, q and t. We obtain almost similar graphs for all irregularity measures which shows that irregularity tends to rise with the increase in the size parameters.

4. Conclusion

The behaviors and tendencies of topological irregularities can be determined by the graph. All graphs exhibit the similar nature of irregularity indices regardless of the particular irregularity index we prefer to study the irregularity of the cerium oxide. This graphical analysis can be used to model new nanostructures where irregularities can be controlled by controlling involved parameters. Using these graphs and above table of values, the estimate of properties of cerium oxide can be done. Due to the lack of resources regarding wet lab, we pose it as an open problem to give some families of hydrocarbons whose complexity depend on irregularity indices as has been done in (Gutman, 2018; Reti et al., 2018).

Author contributions

M.M. gave the idea, H.A. wrote the article and Jia-Bao Liu and Qi Zhang edited and verified the results.

Data availability statement

No such data has been used for this study.

Acknowledgements

References

Abdo, H., Dimitrov, D., 2014. The total irregularity of graphs under graph operations. Miskolc Math. Notes 15, 3–17.

Abdo, H., Dimitrov, D., 2014. The irregularity of graphs under graph operations. Discuss. Math. Graph. Theory 34, 263–278.

Abdo, H., Brandt, S., Dimitrov, D., 2014. The total irregularity of a graph. Discr. Math. Theor. Comput. Sci. 16, 201–206.

Albertson, M., 1997. The irregularity of a graph. Ars Comb. 46, 219–225.

Behzad, M., Chartrand, G., 1947. No graph is perfect. Am. Math. Mon. 74, 962–963.

Bell, F.K., 1992. A note on the irregularity of graphs. Linear Algebra Appl. 161, 45–54.

Brückler, F.M., Došlić, T., Graovac, A., Gutman, I., 2011. On a class of distance-based molecular structure descriptors. Chem. Phys. Lett. 503, 336–338.

Chartrand, G., Erdos, P., Oellermann, O., 1988. How to define an irregular graph. Coll. Math. J. 19, 36–42.

Collatz, L., Sinogowitz, U., 1957. Spektren endlicher Graphen. Abh. Math. Sem. Univ. Hamburg 21, 63–77.

Deng, H., Yang, J., Xia, F., 2011. A general modeling of some vertex-degree based topological indices in benzenoid systems and phenylenes. Comp. Math. Appl. 61, 3017–3023.

Estrada, E., 2010 Sep. Randić index, irregularity and complex biomolecular networks. Acta Chim Slov. 57 (3), 597–603. PMID: 24061806.

Gao, W., Abdo, H., Dimitrov, D., 2017. On the irregularity of some molecular structures. Can. J. Chem. 95, 174–183. https://doi.org/10.1139/cjc-2016-0539.

Gao, W., Aamir, M., Iqbal, Z., Ishaq, M., Aslam, A., 2019. On Irregularity Measures of Some Dendrimers Structures. Mathematics 7, 271.

Gutman, I., 2018. Topological Indices and Irregularity Measures. J. Bull. 8, 469–475.

Horoldagva, B., Buyantogtokh, L., Dorjsembe, S., Gutman, I., 2016. Maximum size of maximally irregular graphs. Match Commun. Math. Comput. Chem. 76, 81–98.

Hu, Y., Li, X., Shi, Y., Xu, T., Gutman, I., 2005. On molecular graphs with smallest and greatest zero[th]-Corder general randic index. MATCH Commun. Math. Comput. Chem. 54, 425–434.

Hussain, Z., Munir, M., Rafique, S., Hussnain, T., Ahmad, H.C., Kwun, Y.M., Kang, S., 2019. Imbalance-Based Irregularity Molecular Descriptors of Nanostar Dendrimers. Processes 7, 517. https://doi.org/10.3390/pr7080517.

Hussain, Z., Rafique, S., Munir, M., Athar, M., Chaudhary, M., Ahmad, H., Min, K.S., 2019. Irregularity molecular descriptors of hourglass, jagged-rectangle, and triangular benzenoid systems. Processes. 7, 413.

Hussain, Z., Yang, Y., Munir, M., Hussain, Z., Athar, M., Ahmed, A., Ahmad, H., 2020. Analysis of irregularity measures of zigzag, rhombic, and honeycomb benzenoid systems. Open Physics 18 (1), 1146–1153. https://doi.org/10.1515/phys-2020-0194.

Klavžar, S., Gutman, I., 1996. A Comparison of the Schultz molecular topological index with the Wiener index. J. Chem. Inf. Comput. Sci. 36, 1001–1003.

Liu, F., Zhang, Z., Meng, J., 2014. The size of maximally irregular graphs and maximally irregular triangle–free graphs. Graphs Comb. 30, 699–705.

Majcher, Z., Michael, J., 1997. Highly irregular graphs with extreme numbers of edges. Discr. Math. 164, 237–242.

Reti, T., Sharfdini, R., Dregelyi-Kiss, A., Hagobin, H., 2018. Graph irregularity indices used as molecular descriptors in QSPR studies. MATCH Commun. Math. Comput. Chem. 79, 509–524.

Ribeiro, A.N., Ferreira, N.D.S., 2017. Systematic study of the physical origin of ferromagnetism in CeO2_ δ nanoparticles. Physical Review B 95 (14), 144–150.

Rucker, G., Rucker, C., 1999. On topological indices, boiling points, and cycloalkanes. J. Chem. Inf. Comput. Sci. 39, 788–802.

Sayle, T.X.T., Parker, S.C., Catlow, C.R.A., 1994. The role of oxygen vacancies on ceria surfaces in the oxidation of carbon monoxide. Surface Science 316 (3), 329–336.

Tseng, E.N., Hsiao, Y.T., Chen, Y.C., Chen, S.Y., Gloter, A., Song, J.M., 2019. Magnetism and plasmatic performance of macroscopic hollow ceria spheres decorated with silver nanoparticles. Nanoscale 11 (8), 3574–3582.

Vukičević, D., Graovac, A., 2004. Valence connectivities versus Randić, Zagreb and modified Zagreb index: A linear algorithm to check discriminative properties of indices in acyclic molecular graphs. Croat. Chem. Acta 77, 501–508.

Wu, X., Neil, C.W., Kim, D., Jung, H., Jun, Y.S., 2018. Co-effects of UV/H2O2 and natural organic matter on the surface chemistry of cerium oxide nanoparticles. Environmental Science: Nano 5 (10), 2382–2393.

S. Yalcin, B. Aktas, D. Yilmaz, Radiation shielding properties of Cerium oxide and Erbium oxide doped obsidian glass, Radiation Physics and Chemistry, 2019, 160, 83-88, ISSN 0969-806X..

Yang, B., Munir, M., Rafique, S., Ahmad, H., Liu, J.-B., 2019. Computational Analysis of Imbalance-Based Irregularity Indices of Boron Nanotubes. Processes 7, 678. https://doi.org/10.3390/pr7100678.

Yılmaz, D., Aktaş, B., Yalçın, S., Albaşkara, M., 2020. Erbium oxide and Cerium oxide-doped borosilicate glasses as radiation shielding material. Radiation Effects and Defects in Solids 175 (5–6), 458–471. https://doi.org/10.1080/10420150.2019.1674301.

Zahid, I., Aslam, A., Ishaq, M., Aamir, M., 2019. Characteristic study of irregularity measures of some Nanotubes. Can. J. Phys.. https://doi.org/10.1139/cjp-2018-0619.